Stability, reusability, and equivalent circuit of TiO2/treated metakaolinite-based dye-sensitized solar cell: effect of illumination intensity on Voc and Isc values

Winda Rahmalia, Imelda Silalahi, Thamrin Usman, Jean-François Fabre, Zéphirin Mouloungui, Georges Zissis

Materials for Renewable and Sustainable Energy (2021) 10:10
https://doi.org/10.1007/s40243-021-00195-9

ORIGINAL PAPER

Stability, reusability, and equivalent circuit of TiO_2/treated metakaolinite-based dye-sensitized solar cell: effect of illumination intensity on V_{oc} and I_{sc} values

Winda Rahmalia[1] · Imelda H. Silalahi[1] · Thamrin Usman[1] · Jean-François Fabre[2] · Zéphirin Mouloungui[2,4] · Georges Zissis[3]

Received: 24 July 2020 / Accepted: 31 May 2021 / Published online: 3 June 2021

Abstract
In this research, treated metakaolinite (TMK) was introduced into the TiO_2 photoelectrode to fabricated dye-sensitized solar cells (DSSCs). The photovoltaic cells have four main natural components, i.e., a photosensitizer (carotenoid bixin), photoelectrode (TiO_2/kaolinite), electrolyte (glycerine carbonate derivative), and counter-electrode (carbon). Their stability, reusability, and equivalent circuit were studied. The presence of 5% of TMK in anatase TiO_2 paste decreased the TiO_2 band gap from 3.21 to 3.16 eV. The result showed that the presence of 5% of TMK in TiO_2 paste was more favorable to obtain higher energy conversion efficiency. Under a light intensity of 200 W/m^2, it produced an energy conversion yield of 0.086%. The combination of the electrolyte and the TMK demonstrated a synergistic effect to improve the electrical properties of the DSSC. The energy storage function worked well until the third day of analysis. The DSSC based on TiO_2/TMK photoelectrode exhibited 16 times better stability than pure TiO_2-based photoelectrode. The Faraday charge transfer processes showed that the TiO_2/TMK photoelectrode is not in direct contact with the carbon counter-electrode.

Keywords Bixin · Dye-sensitized solar cell · Equivalent circuit · Metakaolinite · Photoelectrode

Introduction

Dye-sensitized solar cells (DSSCs) are a third-generation photovoltaic cell that converts any visible light into electrical energy. However, ruthenium and several materials used in these cells are toxic and relatively expensive because they have a low natural abundance. They offer a promising alternative to conventional and expensive silicon-based solar cells [1–3]. Electrical energy is generated when they are exposed to light. Electrons in dye molecules are excited and then injected into a semiconductor photoelectrode (TiO_2, ZnO, WO, etc.) conduction band, where dye molecules adsorb. These electrons migrate through the host semiconductor particles until they reach the collector, then the holes simultaneously generated are reduced by a redox electrolyte or hole carrier at the counter-electrode (Pt, carbon, etc.). This cycle is well regenerative since no substance has been consumed or produced during the process. However, some reactions may occur and cause a significant decrease in the effectiveness of the DSSCs. They are the recombination of the electrons injected either with the oxidized sensitizer or with the oxidized redox couple on the surface of photoelectrode [2, 4].

Several studies have reported that SiO_2 and Al_2O_3 are an energy barrier for suppressing charge recombination due to their insulation properties [5–7]. They can decrease the interaction between the excited electrons in the photoelectrode and the electrolyte ions [8]. Synthetic nanoclay has been used to solidify a liquid electrolyte and induce a light scattering, increasing the overall light absorption, especially

✉ Winda Rahmalia
winda.rahmalia@chemistry.untan.ac.id

1 Department of Chemistry, Faculty of Mathematics and Natural Science, Universitas Tanjungpura, Jl. Prof. Dr. H. Hadari Nawawi, Pontianak 78124, West Kalimantan, Indonesia

2 Laboratoire de Chimie Agro-Industrielle, ENSIACET-INPT, Université de Toulouse, 4 allée Emile Monso, 31030 Toulouse, France

3 Laboratoire Plasma et Conversion d'Energie, LAPLACE, Université de Toulouse III-Paul Sabatier, 118 route de Narbonne-Bât3R3, 31062 Toulouse, France

4 INRA, UMR 1010 CAI, 31030 Toulouse, France

in the red region [9–11]. Many clays have been also developed as supporting materials for photocatalytic application [12–14]. The application of natural clay for the photoelectrode in DSSCs has been scarcely reported. Saelim et al. [15] applied TiO_2/modified natural bentonite clay photoelectrode for DSSCs. However, TiO_2/clay photoelectrode provided a lower DSSC efficiency than the pure TiO_2 photoelectrode, probably due to the high composition of clay used.

We previously reported the characteristic of treated kaolinite and metakaolinite compared with the natural kaolinite (NK). Their X-ray diffraction (XRD), Fourier-transform infrared spectroscopy (FTIR), scanning electron microscopy–energy-dispersive spectroscopy (SEM–EDS), and Brunauer–Emmett–Teller (BET) analysis data have been reported [16]. Based on that previous study, NH_4OH-treated metakaolinite (TMK) has certain advantages over NK: (1) TMK has a BET specific surface area of 124.33 m^2/g, 16 times greater than NK (7.65 m^2/g). (2) It also has the highest Si/Al ratio (2.06), 2 times greater than NK (1.26). Their interaction with bixin has also been investigated [16, 17]. This paper presents the role of TMK in small concentrations in the TiO_2 photoelectrode for DSSCs.

We used bixin (methyl hydrogen 9′-*cis*-6,6′-diapocarotene-6,6′-dioate) as presented in Fig. 1 as a natural sensitizer. It is a pigment in the apocarotenoids group obtained from annatto seeds (*Bixa orellana* L.) [18]. It carries a carboxylic group at one end and a carboxyester group at the second end of the hydrocarbon chain. This functional group allows bixin to be easily bonded to the photoelectrode surface and facilitates the injection of electrons into the photoelectrode conduction band. Bixin has absorption coefficients in aprotic polar solvents of more than 10^4 M^{-1} cm^{-1} which is an advantage of dyes as sensitizers in the DSSCs [19–21]. The bio-sourced carbonate solvents suitable for the redox I^-/I_3^- pair have also been developed. Besides that, in this study, we use a mesoporous carbon-based counter-electrode which will allow the DSSCs generated to be environmentally friendly. As it has been known that the existing DSSC common component consists of toxic materials and relatively expensive because they have a low natural abundance. These materials are ruthenium as a sensitizing dye, an electrolyte containing a redox couple in acetonitrile, and a platinum-based counter-electrode [1–3].

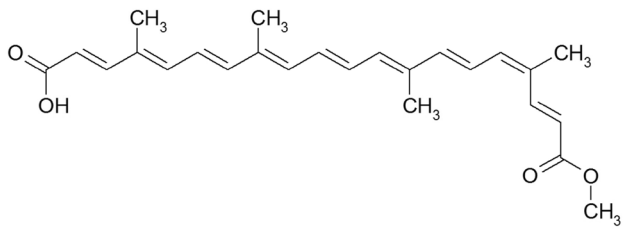

Fig. 1 *Cis*-bixin structure

Two of the keys parameters which govern the attainable power from a DSSC are the open-circuit voltage (V_{oc}) and circuit current (I_{sc}). The V_{oc} is the maximum voltage available from a solar cell that occurs at zero current, while I_{sc} is the current through the solar cell when the voltage across the solar cell is zero. For long-term usage, both physical and chemical stability and reusability should be considered. The model of an equivalent circuit of DSSC allows for obtaining a cell network, simulating the system, and contributing to the implied electric processes analysis. For these reasons, the results presented in this paper are related to the studies carried out on these parameters, which are influenced by direct illumination intensity.

Materials and methods

Materials

Bixin crystals containing 88.11% *cis*-bixin and 11.75% di-*cis*-bixin and an unknown compound (0.14%) were obtained from the extraction and purification processes Rahmalia et al. [22]. Glycerol carbonate acetate (GCA) were obtained by acyl transfer reaction by acylation of glycerol carbonate by acetic anhydride catalyzed by cation-exchange resins. GCA were purified by the fine film separator. The properties of GCA: N°CAS 1607-31-4; density at 25 °C 1.296; dipole moment (*D*) 6.19; dielectric constant (ε) 47.8; boiling point, mm Hg (°C) 330; melting point (°C) − 62.5; flashpoint (°C) 176 [23].

Natural kaolinite (CAS Number 1318-74-7), anatase TiO_2 nanopowder (CAS Number 1317-70-0), carbon mesoporous (CAS Number 1333-86-4), and all analytical reagent (ammonium hydroxide ≥ 25% CAS Number 1336-21-6, isopropanol 99.5% CAS Number 67-63-0, acetylacetone ≥ 99% CAS Number 123-54-6, triton™ X-100 CAS Number 9002-93-1, ethanol absolute CAS Number 64-17-5, and dimethyl carbonate 99% CAS Number 105-58-8) were supplied by Sigma-Aldrich, Germany. Fluorine-doped tin oxide (FTO)-coated TEC-7 conductive glasses (the material: SnO_2/F, the typical layer thickness: 600 nm, the square resistance: 6–8 Ω, the total transmission at 400–800 nm: 70–81%) were provided by SOLEM.

Methods

Preparation of treated metakaolinite

The natural kaolinite (NK) was calcined at 600 °C in a furnace for 6 h to form metakaolinite (MK). An amount of 10 g of MK was added to 100 mL 5 M NH_4OH. The mixtures

were incubated at room temperature for 6 h, with constant shaking (300 rpm). The suspension was filtered. The residue was washed with distilled water until neutral and dried in an oven at 103 °C for 24 h. This process was repeated three times to optimize activation. The final product obtained was called TMK [17].

Preparation of photoelectrode

The photoelectrode was prepared on a space of 0.5 cm^2 by the method of doctor blading as follows [19]. The FTO substrates were sonicated in a mixture of deionized water and isopropanol (1:1 v/v) for 1 h. Clean FTO substrates were heated at 450 °C for 30 min before film deposition.

TiO_2 paste was first prepared by adding 2.5 g of TiO_2, 16 drops of acetylacetone, and 12 drops of triton™ X-100 to 20 mL of ethanol absolute, and was stirred at 200 rpm in a magnetic stirrer for 72 h until a paste formed. To make TMK-modified TiO_2 photoelectrodes, TMK was applied with different concentrations concerning the mass of TiO_2 (0, 3, 5, 7, and 10% w/w) in the paste. The TiO_2 paste was then applied on FTO by the doctor blading method using magic tape as a masking material, was air dried, and heated at 500 °C for 1 h. After cooling to 50 °C, the electrode was taken out of the oven. It was immersed in a solution of bixin diluted in dimethyl carbonate for 24 h. The concentration of the bixin used was 1.33 g/L.

Cell assembly

DSSC assembled as a sandwich structure. The carbon paste was utilized as a counter-electrode. It was prepared by adding 640 mg carbon mesoporous, 1 mL of photoelectrode paste, and 1 mL of triton x-100 into 2 mL of demineralized water. The mixture was mixed under ultrasound 20 kHz for 5 min. The carbon paste was also coated on TCO by the doctor blading method using magic tape as a masking material, air dried, and heated at 250 °C for 1 h. A drop of electrolyte composed of 404 mg of KI, 261 mg of I_2, and 551 mg of glycerol carbonate acetate, was introduced onto the cells. Finally, the cell was assembled using epoxy glue (Fig. 2). The cells produced are called TiO_2/Bx/KI-I_2 + GCA/C, TiO_2 + 3%TMK/Bx/KI-I_2 + GCA/C, TiO_2 + 5%TMK/Bx/KI-I_2 + GCA/C, TiO_2 + 7%TMK/Bx/ KI-I_2 + GCA/C, and TiO_2 + 10%TMK/Bx/ KI-I_2 + GCA/C for the use of 0, 3, 5, 7 and 10% of TMK, respectively, in the TiO_2 paste. We prepared different redox couples (KI-I_2 and LiI-I_2 separately) in GCA to study electrolyte type effects.

Measurement of DSSCs performance

DSSCs performance was measured using a 50-W xenon lamp (PRO-LITE), and the intensity was measured using a multimetric SPM72 solar meter. The distance between the light and the DSSC was 20 cm, and the intensity of the lamp was adjusted using a lighting control dimmer. The V_{oc} and I_{sc} generated by DSSC under varying intensities (0–1000 W/m^2 ignoring the effect of the temperature) were determined using an Agilent 34461A multimeter equipped with Keysight BenchVue software. Measurement of I_{sc} and V_{oc} produced by DSSCs at each light intensity was carried out for 3 min. The equivalent circuits of DSSCs were determined using an AMETEX solartron equipped with Modulab MTS software.

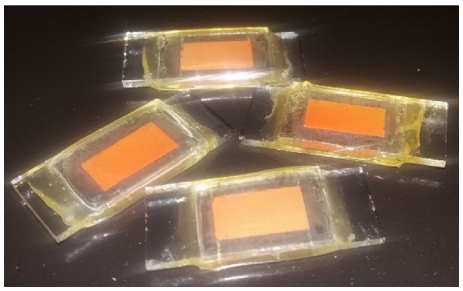

Fig. 2 Assembled bixin-sensitized solar cell

Result and discussion

Characterization results of kaolinites and prepared photoelectrode

This research used the anatase crystalline phase of TiO_2 because it is an indirect band gap semiconductor and can favor electron transport and diffusion of electrolyte species, directly impacting solar cell efficiency [24, 25]. The absorption spectra (Fig. 3a) were used to determine the optical properties of the pure TiO_2 and TMK-modified TiO_2-based photoelectrodes. The absorption spectrum fitting method using Tauc model was applied to estimate their optical band gap [26]. The calculated band gap of pure TiO_2-based photoelectrode is 3.21 eV (Fig. 3b), corresponding to their absorbance at 387 nm in the ultraviolet region of the solar spectrum and consistent with the reported results [24, 26]. The band gap of TiO_2 + 3%TMK, TiO_2 + 5%TMK, TiO_2 + 7%TMK, and TiO_2 + 10%TMK photoelectrode are approximately 3.17 (392 nm), 3.16 (393 nm), 3.20 (388 nm), and 3.21 (387 nm), respectively (Fig. 3). All of the photoelectrodes yielded band gap values that were very close together, around 3.21–3.16 eV. However, there was an effect of concentration on the band gap values, and it is evident that there is a slight shift in the adsorption towards the visible region for TiO_2 + 3%TMK-, TiO_2 + 5%TMK-based photoelectrodes. The observed shift is due to the transfer of charge carriers between the TMK and the TiO_2 conduction or valence band.

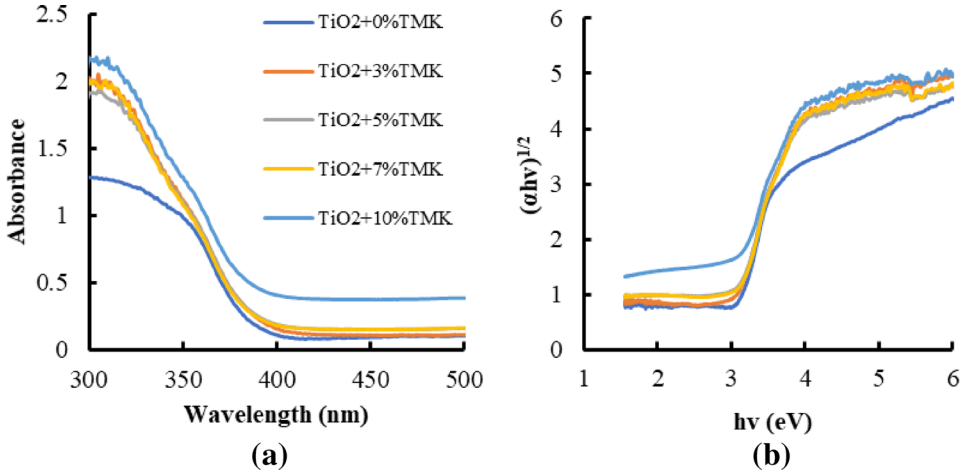

Fig. 3 Absorption spectra (**a**) and absorption spectrum fitting method using Tauc model of TiO_2/TMK photoelectrodes

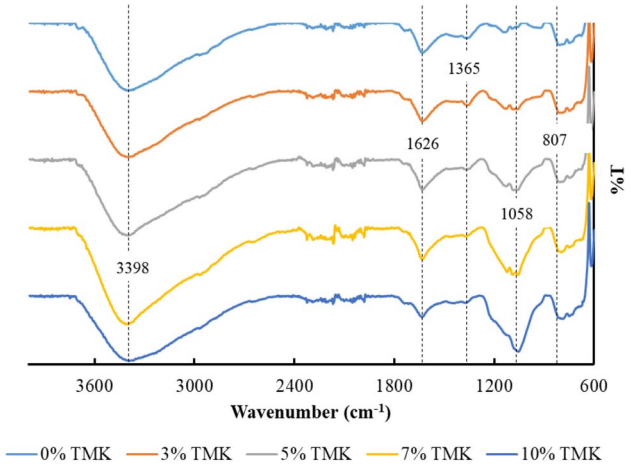

Fig. 4 FTIR spectra of TiO_2/TMK-based photoelectrodes

Functional groups in DSSC photoelectrodes due to the addition of TMK were analyzed using FTIR. Figure 4 shows that FTIR spectrum of TiO_2 photoelectrode characteristic bands of: at 3398 cm^{-1} corresponds to stretching of the hydroxyl group of water, 1626 cm^{-1} corresponds to the O–H deformation, and 1365 cm^{-1} corresponds to stretching vibration of Ti–O–Ti and O–Ti–O. For TMK-modified TiO_2 photoelectrodes, the peak at 1058 cm^{-1} is assigned to the skeleton Si–O stretching vibration of the network (Si–O–Si and O–Si–O). This peak is not observed in the FTIR spectrum of pure TiO_2-based photoelectrode. The detection of O–Ti–O and O-Si–O bonds in the TiO_2/TMK-based photoelectrodes can support the hypothesis that the increase in energy conversion yield was influenced by these functional groups, which can facilitate the chemical adsorption of the bixin on the photoelectrode surface.

Effect of illumination intensity on V_{oc} and I_{sc} values of DSSC

Figure 5 shows the parameters affecting DSSCs performance using TiO_2/TMK-based photoelectrodes with different concentrations of TMK. As shown in Fig. 5, V_{oc} and I_{sc} increase logarithmically with light intensity. All DSSCs have the same curve pattern. TMK played an essential role in the performance of DSSCs. The V_{oc} generated by TiO_2/Bx/KI-I_2 + GCA/C is higher than that of TiO_2 + 3%TMK/Bx/KI-I_2 + GCA/C, TiO_2 + 7%TMK/Bx/KI-I_2 + GCA/C, and TiO_2 + 10%TMK/ Bx/KI-I_2 + GCA/C, but lower than that of TiO_2 + 5%TMK/Bx/KI-I_2 + GCA/C. It could be related to the optical energy gap value (E_g) of anodes. Lower energy gap to be responsible the enhancement of electron injection and transport. The TiO_2 + 5%TMK/Bx/KI-I_2 + GCA/C has the highest V_{oc}, and this shows that 5% of TMK added to the photoelectrode paste is the optimum concentration of TMK to apply in these works.

Overall, the intervention TMK in the TiO_2 photoelectrode has a significant effect on the increase of the I_{sc}. DSSC used TiO_2/TMK photoelectrode to show higher I_{sc} relative to DSSC used pure TiO_2 photoelectrode. The percentage increase in TMK more than 5% decreases the I_{sc} slightly. Since the insulating properties of SiO_2 and Al_2O_3, they can function as a barrier to energy by removing the recharge. In this case, TMK will reduce the interaction between the excited electrons of bixin in the TiO_2 photoelectrode and the electrolyte ions [6, 7, 15].

DSSC used TiO_2/TMK photoelectrode show the highest peak efficiency under 200 W/m^2 illumination. The energy conversion yield is higher than that of DSSCs with pure TiO_2. Under these conditions, TiO_2/Bx/KI-I_2 + GCA/C, and TiO_2 + 3%TK5/Bx/KI-I_2 + GCA/C, TiO_2 + 5%TK5/Bx/KI-I_2 + GCA/C, TiO_2 + 7%TK5/Bx/KI-I_2 + GCA/C, and TiO_2 + 10%TK5/Bx/ KI-I_2 + GCA/C show efficiencies 0.021, 0.014, 0.050, 0.015, and 0.013%, respectively.

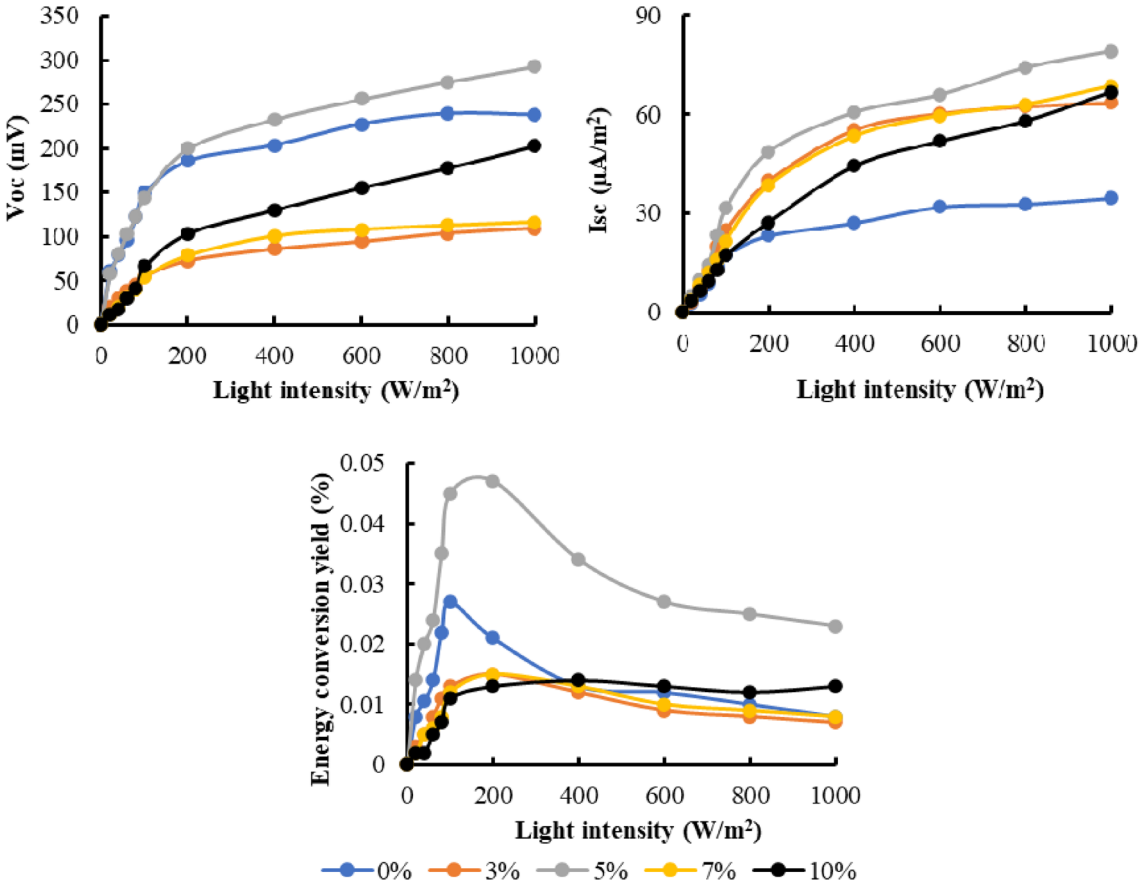

Fig. 5 Parameters affecting DSSCs performance using TiO_2/TMK-based photoelectrodes with different concentrations of TMK

Under 100 W/m^2 of light intensity, the efficiency obtained by TiO_2 + 5%TK5/Bx/KI-I_2 + GCA/C is also higher than that of TiO_2/Bx/KI-I_2 + GCA/C.

A redox couple is a critical element in the liquid electrolyte. Its functions concern the regeneration of the dye and the charge transport between the two electrodes, playing a crucial role in determining the photovoltaic performance of DSSCs. The redox couple of I^-/I_3^- was used as a redox couple at the beginning of the DSSCs research work. It has proven to be one of the most versatile redox couples. Overall, I^-/I_3^- pair has good solubility, does not absorb too much light, has an appropriate redox potential, and allows rapid dye regeneration [1, 27, 28].

In this research, we compared LiI- and KI-based redox couples, resulting in TiO_2 + 5%TMK/Bx/KI-I_2 + GCA/C and TiO_2 + 5%TMK/Bx/LiI-I_2 + GCA/C. The performance comparisons of these cells are shown in Fig. 6. Under different light intensities, TiO_2 + 5%TMK/Bx/KI-I_2 + GCA/C and TiO_2 + 5%TMK/Bx/LiI-I_2 + GCA/C produce an almost similar value of V_{oc}, indicated by the coinciding curve. This phenomenon was in agreement with the study results by Lee et al. [29], who reported that V_{oc} was influenced by the amount of dye adsorbed on the surface of the photoelectrode. Since the same photoelectrode composition was used, the amount of bixin absorbed on the surface of the photoelectrode of the two cells and facilitating the harvesting of photons was almost the same.

However, TiO_2 + 5%TMK/Bx/LiI-I_2 + GCA/C shows the higher I_{sc} relative to that of TiO_2 + 5%TMK/Bx/KI-I_2 + GCA/C. Consider the smaller radius of Li^+ cation that causes its diffusion coefficient higher than K^+. The Li^+ cations had better adsorption on the TiO_2/electrolyte surface when compared to K^+ cations [28]. Tsai et al. [30] reported that LiI improves I_{sc}. The LiI molecule decomposes to Li^+ when it is adsorbed on the TiO_2 surface by attracting electrons from the conduction band. Our results show that LiI-I_2-based redox couples can improve the performance of DSSC with an efficiency up to 0.062%, which is higher than that of DSSC fabricated with KI-I_2 based redox couple 0.050%.

Generally, the I^-/I_3^- ratio in the electrolyte of a DSSC is adjusted to achieve the highest PV performance. During electricity generation in a DSSC, I^- is oxidized to I_3^- by the sensitizer in the photoelectrode, whereas I_3^- is reduced to I^- on the counter-electrode. Therefore, the I^-/I_3^- ratio

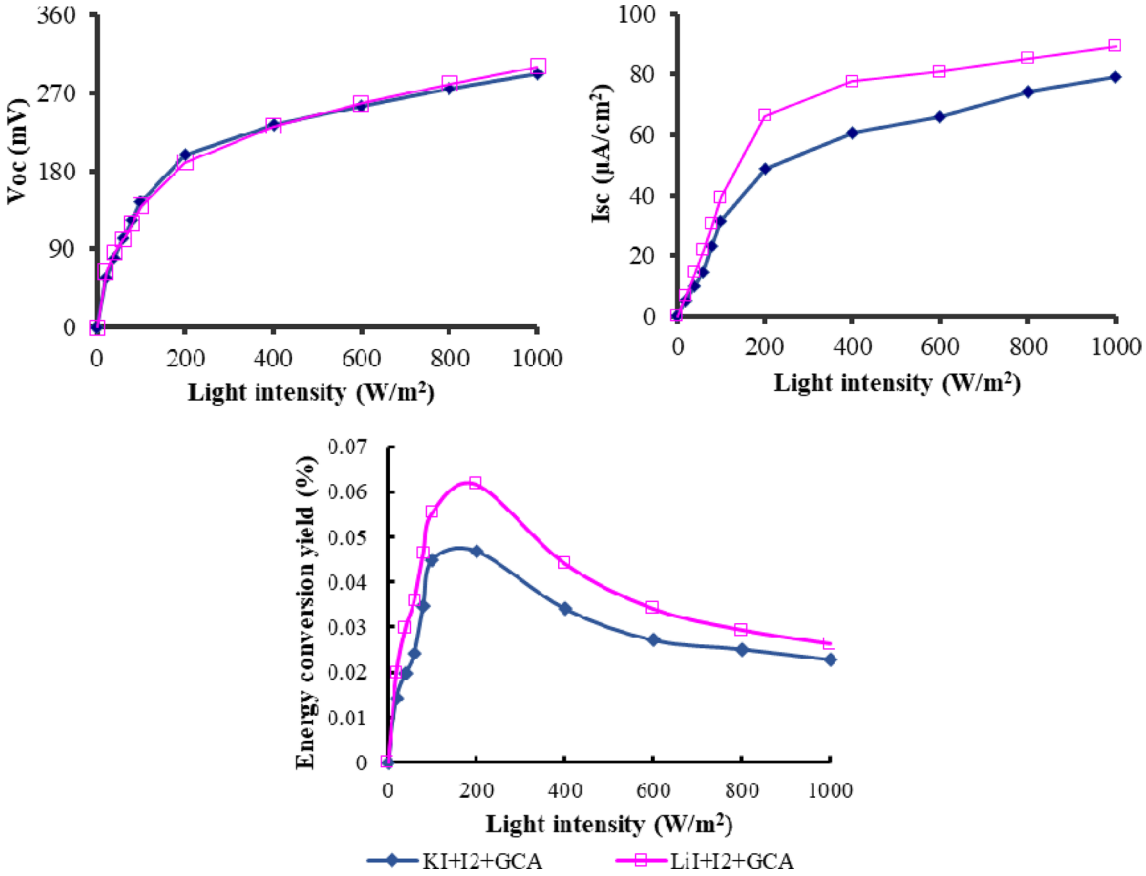

Fig. 6 Parameters affecting the performance of the DSSCs using the different redox couples

remains constant during electricity generation. However, when the forward current continues to flow in the DSSCs, I^- is not sufficiently oxidized in the photoelectrode, causing the I^-/I_3^- ratio to increase and the current characteristics to change [31]. Because of these reasons, we also optimized LiI and I_2 composition in GCA-based electrolytes. The results are shown in Fig. 7. In the following discussion, we will use the terms TiO_2 + 5%TMK/Bx/LiI-I_2 + GCA-1/C, TiO_2 + 5%TMK/Bx/LiI-I_2 + GCA-2/C and TiO_2 + 5%TMK/Bx5/LiI-I_2 + GCA-3/C for use of 350:1, 250:1, and 150: 1 in mol ratio of LiI:I_2 in GCA.

Figure 7 shows that LiI-I_2 ratios in the electrolyte have a great influence on the performance of DSSC. A decrease in I_{sc} and V_{oc} was observed using a larger percentage of LiI so that in this study, TiO_2 + 5%TMK/Bx/LiI-I_2 + GCA-3/C showed the best performance. This observation may be due to the ion-pair formation of ion pairs and cross-linking sites that impede the movement of ions in GCA and reduce ion mobility. Under 200 W/m^2 of light intensity, TiO_2 + 5%TMK/Bx/LiI-I_2 + GCA-1/C, TiO_2 + TMK/ Bx/LiI-I_2 + GCA-2/C and TiO_2 + 5%TMK/Bx/LiI-I_2 + GCA-3/C efficiencies of 0.039, 0.062, and 0.086%, respectively.

Stability and reusability of the DSSCs

To investigate the role of TMK in DSSCs stability and reproducibility, we examined two DSSCs fabricated with the optimal conditions. One of DSSC with TiO_2/TMK photoelectrode (cell A) and the other one of cell with pure TiO_2 photoelectrode (cell B). Both of cells are illuminated continuously for 7 h under 200 W/m^2 of light intensity. The ability of these cells to recover energy (reusability) was also investigated. For this purpose, after 7 h of illumination, the cells are stored in the dark for 17 h. We repeated this operation for three days. Changes in the performance parameters of the DSSCs are presented in Fig. 8.

Figure 8 shows cell A produces V_{oc}, I_{sc}, and energy conversion yields are higher than those of cell B. This phenomenon is consistent with the results presented previously. On the first and second days, according to this figure, the two cells need 10 min of illumination time to reach the maximum value of I_{sc}. After 10 min, the considerable decrease in V_{oc} and I_{sc} results in decreased energy conversion yield for both cells. We assume that the initial increase in energy conversion yield can be attributed to photoinduced annealing, then improving overall

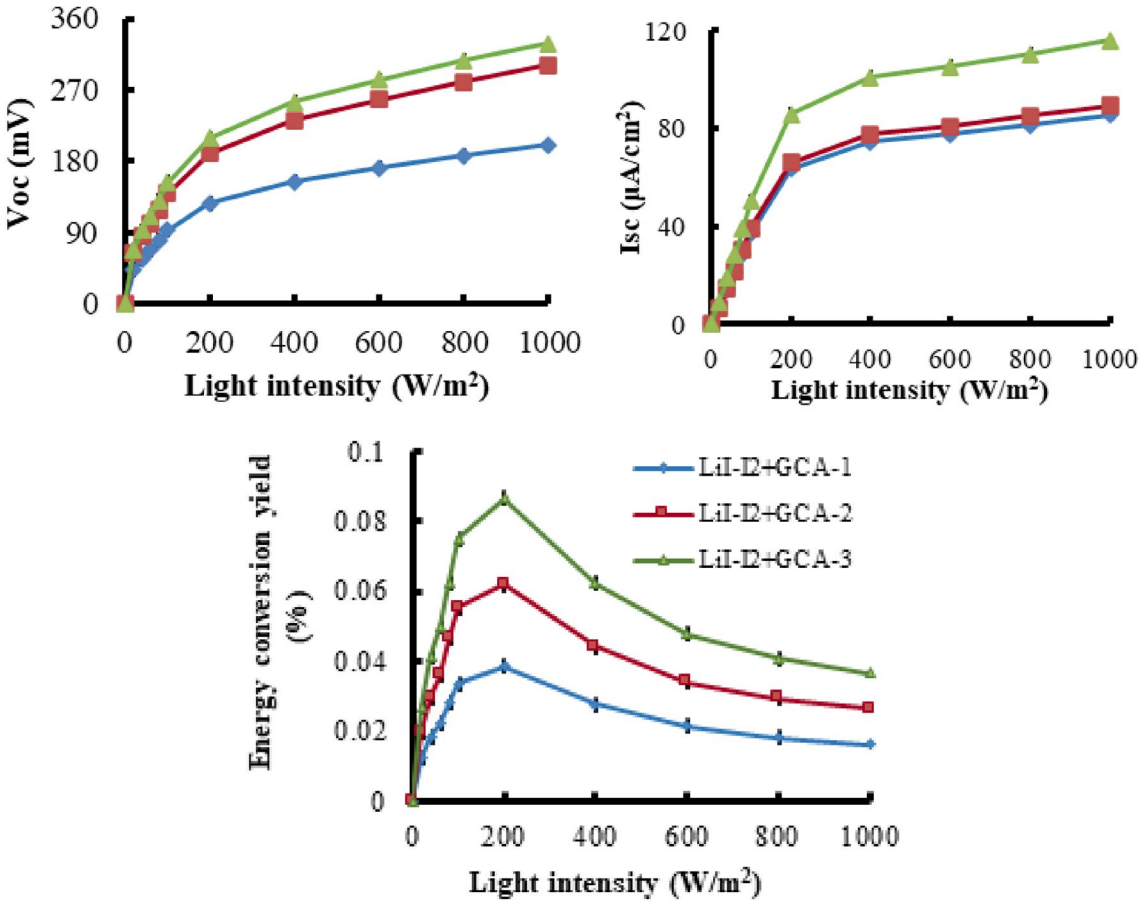

Fig. 7 Parameters affecting the performance of the DSSCs using the LiI-I_2-based redox couple in the different compositions

performance. This can occur, for example, by recovering and/or rearranging some of the dangling or taut bonds between the dye and the photoelectrode or within the dye molecules [31]. Under these circumstances, the decrease in voltage changes much more than the current.

The data also showed that the two cells assembled are reusable. They could recover their energy after being rested for 17 h. Their energy storage and charging function worked well until the third day. However, by the third day, cell B can recover less energy compared to cell A. This is shown by the initial value of I_{sc} and V_{oc}, which fall sharply and fall below the second day. We calculated kinetics of degradation of cell A and B efficiencies using kinetic models of first (Eq. 1) and second (Eq. 2) order for quantitative analysis. In these analyses, we consider that there is only one factor affecting the decrease in cell yields.

$$\ln R_t/R_0 = -k_1 t, \tag{1}$$

$$1/R_t - 1/R_0 = k_2 t. \tag{2}$$

In these equations, R_0: initial energy conversion yield of the cell, R_t: energy conversion yield of the cell after illumination for t time, k_1: first-order degradation rate constant, and k_2: second-order degradation rate constant. The k_1 and k_2 were calculated from the gradient of the corresponding curve of ln R_t/R_0 vs. t and $1/R_t - 1/R_0$ vs. t. Calculation results are shown in Table 1.

As seen in Table 1, the first- and second-order kinetic equation correlation coefficient values are $r^2 > 0.9$ except the first-order kinetic equation for cell B on the third day. The results confirm that cell B degradation is faster than cell A on the first day, both according to the kinetic model is first order and second order. On the second day, the first-order kinetic model shows that cell A degradation constant is slightly higher than that of cell B, but according to the kinetic model of second order, cell B degradation is always much faster than cell A. Also, for the third day, cell B degradation is 16 times faster than that of cell A. These results

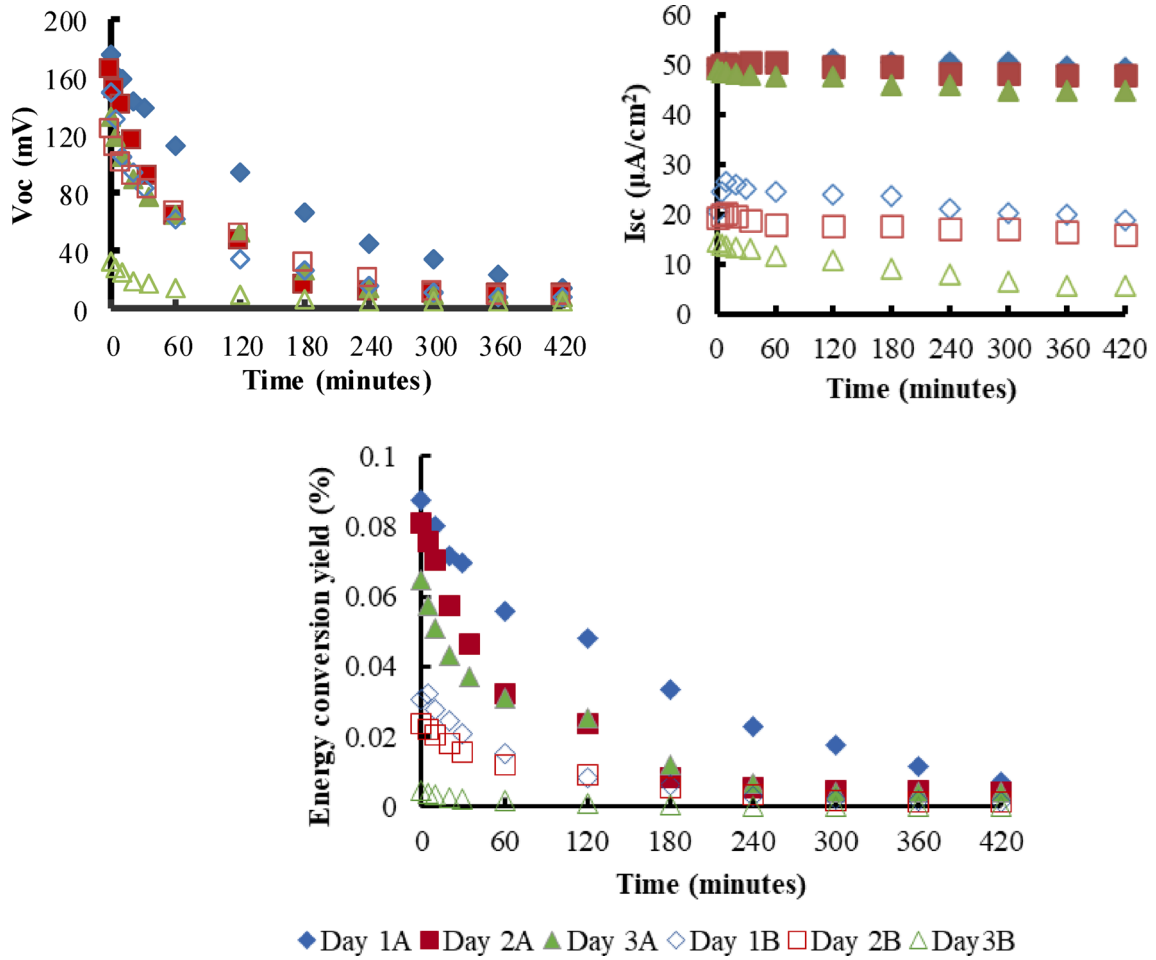

Fig. 8 Changes of performance parameters of TiO_2 + 5%TMK/Bx/LiI-I_2 + GCA-3/C (**A**) and TiO_2/Bx/LiI-I_2 + GCA-3/C (**B**)

Table 1 Kinetic parameters of efficiencies degradation of DSSCs

Cell (day)	Kinetic model of first order		Kinetic model of second order	
	k_1	r^2	k_2	r^2
A (1)	0.0056	0.9929	0.2384	0.8554
B (1)	0.0077	0.9782	1.5177	0.9545
A (2)	0.0078	0.9149	0.5970	0.9537
B (2)	0.0073	0.9904	1.7588	0.9237
A (3)	0.0071	0.9574	0.6121	0.9480
B (3)	0.0019	0.7235	9.7387	0.9801

indicate that the DSSC with TiO_2/TMK photoelectrode is more stable than pure TiO_2-based DSSC. Reusability is significantly better than the CSSB incorporated in the pure TiO_2 photoelectrode.

Equivalent circuit of DSSC

Mathematical modeling of solar cells is essential for any performance optimization operation. An electrochemical cell such as DSSC can be represented by a network of resistors and capacitors known as an equivalent circuit. In this work, the technique of impedance spectroscopy was carried out to analyze the electrochemical phenomena in a DSSC according to Faraday's Law. From an impedance spectrum (drawn in the imaginary plane, or as gain and phase as a function of frequency), it is possible to deduce the equivalent circuit and determine the different elements meaning. This equivalent circuit model of DSSC provides the network of cells and the system simulation and contributes to analyzing the electrical processes involved [32]. Figure 9 shows the impedance spectrum and the corresponding equivalent circuit of the DSSC with TiO_2/TMK photoelectrode (cellA).

Figure 9 schematically illustrates discrete elements of the equivalent circuit of DSSC manufactured in this research conditions. According to this figure, the model system of

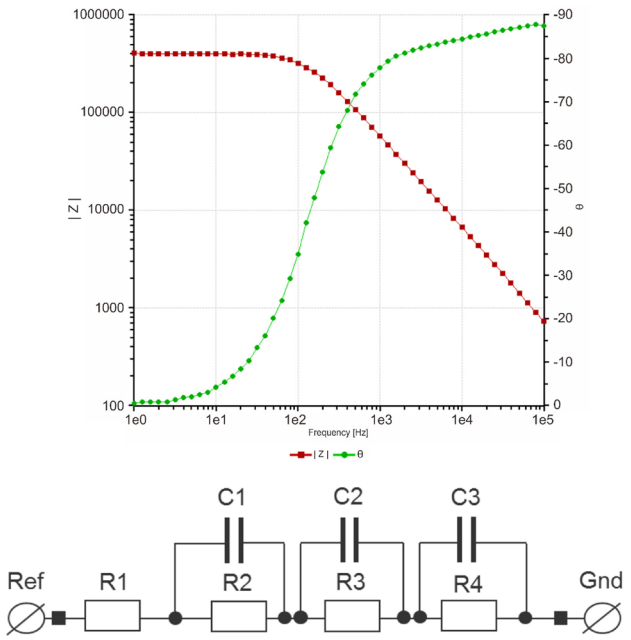

Fig. 9 Impedance spectrum and equivalent circuit of the DSSC with TiO_2/TMK photoelectrode

DSSC introduces a resistance parallel to the capacitance related to the equivalent circuit of the PN junction [33, 34]. It is proved that the TiO_2/TMK photoelectrode is not in direct contact with the counter-electrode of carbon. Since the profile of the DSSC is geometrically symmetrical, we propose some possibilities as follows: towards the TCO, TiO_2/TMK forms an interface with the bixin, it gives the parallel combination of a charge transfer resistance (R2) and a capacitance space charge layer (C1). Therefore, there is no interface between TCO and bixin, and it does not need to be considered. The interface between the TiO_2/TMK and the electrolyte gives another parallel combination (R3 and C2). The same is assumed for the interface between the carbon counter-electrode and the electrolyte that produces R4 and C3. The Faraday charge transfer processes could be summarized in a localized resistance $R_1 = R\ TiO_2$/TMK/bixin + R RTiO$_2$/TMK/electrolyte + R carbon/electrolyte. The DSSC with pure TiO_2 photoelectrode (cell B) shows a similar impedance spectrum pattern and the equivalent circuit.

Conclusions

The results are acceptable in the DSSCs using natural dyes as a sensitizer. The possibility of replacing a portion of TiO_2 with TMK can lead to a considerable reduction in the cost of TiO_2 used. The interaction between TiO_2 and TMK was confirmed from the results of DR-UV and FTIR analysis. Besides that, an appropriate electrolyte composition, which has increased V_{oc} and I_{sc}, has been identified. Means for improving the DSSC energy conversion yield of the TiO_2/TMK electrode should be examined in further studies by optimizing Ti:Si molar ratio and setting the electrode semiconductor preparation process. The presence of TMK in the TiO_2 photoelectrode contributes to improving the performance, stability and reproducibility of the DSSC compared to the DSSC manufactured with the pure TiO_2 photoelectrode. The electrolyte exerts a synergetic effect with the TMK to improve the electrical and conductive parameters of the DSSC.

Acknowledgements This study received financial support from the Ministry of Research Technology and Higher Education Republic of Indonesia (RISTEKDIKTI). We thank Pascal Dupuis (LAPLACE, Université de Toulouse III-Paul Sabatier) for assistance with the analysis of equivalent circuit of DSSC by SOLARTRON.

Declarations

Ethical statements We declare that this paper is original. All authors approve the manuscript and this submission. We have no known competing financial interest or personal relationships that could have appeared to influence the work reported in this paper.

References

1. Grätzel, M.: Dye-sensitized solar cells. J. Photochem. Photobiol. C Photochem. Rev. (2003). https://doi.org/10.1016/S1389-5567(03)00026-1
2. Nazeeruddin, Md.K., Baranoff, E., Grätzel, M.: Dyes-sensitized solar cells: a brief overview. Sol. Energy (2011). https://doi.org/10.1016/j.solener.2011.01.018
3. Semalti, P., Sharma, S.N.: Dye sensitized solar cells (DSSCs) electrolytes and natural photo-sensitizer. J. Nanosci. Nanotech. (2020). https://doi.org/10.1166/jnn.2020.17530
4. Gokilamani, N., Muthukumarasamy, N., Thambidurai, M., Ranjitha, A., Velauthapillai, D.: Grape pigment (malvidin-3-fructoside) as natural sensitizer for dye-sensitized solar cells. Mater. Renew. Sustain. Energy. (2014). https://doi.org/10.1007/s40243-014-0033-6
5. Kumara, G.R.R.A., Tennakone, K., Parera, V.P.S., Konno, A., Kaneko, S., Okuya, M.: Suppression of recombinations in a dye-sensitized photoelectrochemical cell made from a film of tin IV oxide crystallites coated with a thin layer aluminium oxide. J.

Phys. D Appl. Phys. (2001). https://doi.org/10.1088/0022-3727/34/6/306
6. Palomares, E., Clifford, J.N., Haque, S.A., Lutz, T., Durrant, J.R.: Control of charge recombination dynamics in dye-sensitized solar cells by use of conformally deposited metal oxide blocking layers. J. Am. Chem. Soc. (2003). https://doi.org/10.1021/ja027945w
7. Nguyen, T.V., Lee, H.C., Khan, M.A., Yang, O.B.: Electrodeposition of TiO_2/SiO_2 nanocomposite for dye-sensitized solar cell. Sol. Energy (2007). https://doi.org/10.1016/j.solener.2006.07.008
8. Tsui, M.C., Tung, Y.L., Tsai, S.Y., Lan, C.W.: A nano quasi-solid electrolyte with modified nano-clay applied to dye-sensitized solar cells. J. Sol. Energy Eng. (2011). https://doi.org/10.1115/1.4001407
9. Park, J.H., Kim, B.W., Moon, J.H.: Dual functions of clay nanoparticles with high aspect ratio in dye-sensitized solar cells. Electrochem. Solid-State Lett. (2008). https://doi.org/10.1149/1.2957601
10. Costenaro, D., Bisio, C., Carniato, F., Gatti, G., Marchese, L., Oswald, F., Meyer, T.B.: Size effect of syntetic saponite clay in quasi-solid electrolyte for dye-sensitized solar cells (DSSC). Sol. Energ. Mat. Sol. C (2013). https://doi.org/10.1016/j.solmat.2013.05.012
11. He, H., Ren, S., Kong, D., Wang, N.: Improved composite gel electrolyte by layered vermiculite for quasi-solid-state dye-sensitized solar cells. Adv. Cond. Matter Phys. (2014). https://doi.org/10.1155/2014/521493
12. Fatimah, I.: Composite of TiO2-montmorillonite from Indonesia and Its photocatalytic properties in methylene blue and *E. coli* reduction. J. Mater. Environ. Sci. **3**(5), 983–992 (2012)
13. Li, X., Peng, K., Chen, H., Wang, Z.: TiO_2 nanoparticles assembled on kaolinites with different morphologies for efficient photocatalytic performance. Sci. Rep. (2018). https://doi.org/10.1038/s41598-018-29563-8
14. Mishra, A., Mehta, A., Basu, S.: Clay supported TiO_2 nanoparticles for photocatalytic degradation of environmental pollutants: a review. J. Environ. Chem. Eng. (2018). https://doi.org/10.1016/j.jece.2018.09.029
15. Saelim, N., Magaraphan, R., Streethawong, T.: TiO_2/modified natural clay semiconductor as a potential electrode for natural dye-sensitized solar cell. Ceram. Int. (2011). https://doi.org/10.1016/j.ceramint.2010.09.001
16. Rahmalia, W., Fabre, J.F., Usman, T., Mouloungui, Z.: Adsorption characteristics of bixin on acid- and alkali-treated kaolinite in aprotic solvents. Bioinor. Chem. Appl. (2018). https://doi.org/10.1155/2018/3805654
17. Rahmalia, W., Fabre, J.F., Usman, T., Mouloungui, Z.: Preparation of ammonia dealuminated metakaolinite and its adsorption against bixin. Indones. J. Chem. (2020). https://doi.org/10.22146/ijc.44706
18. Giuliano, G., Rosati, C., Bramley, P.M.: To dye or not to dye: biochemistry of annatto unveiled. Trends Biotechnol. (2003). https://doi.org/10.1016/j.tibtech.2003.10.001
19. Gómez-Ortíz, N.M., Vázquez-Maldonado, I.A., Pérez-Espadas, A.R., Mena-Rejón, G.J., Azamar-Barrios, J.A., Oskam, G.: Dye-sensitized solar cells with natural dyes extracted from Achiote seeds. Sol. Energy Mater. Sol. Cells (2010). https://doi.org/10.1016/j.solmat.2009.05.013
20. Hiendro, A., Hadary, F., Wahyuni, N., Rahmalia, W.: Enhanced performance of bixin-sensitized TiO_2 solar cells with activated kaolinite. Int. J. Eng. Res. Innov. (2012). https://doi.org/10.1109/ESciNano.2012.6149642
21. Rahmalia, W., Fabre, J.F., Usman, T., Mouloungui, Z.: Aprotic solvents effect on the UV–visible absorption spectra of bixin. Spectrochim. Acta A. (2014). https://doi.org/10.1016/j.saa.2014.03.119
22. Rahmalia, W., Fabre, J.F., Mouloungui, Z.: Effect of cycloexane/acetone ratio on bixin extraction yield by accelerated solvent extraction method. Proc. Chem. (2015). https://doi.org/10.1016/j.proche.2015.03.061
23. Mouloungui, Z., Pelet, S.: Study of the acyl transfer reaction: structure and properties of glycerol carbonate esters. Eur. J. Lipid Sci. Technol. (2001). https://doi.org/10.1002/1438-9312(200104)103:43.3.CO;2-A
24. González-Verjan, V.A., Trujillo-Navarrete, B., Félix-Navarro, R.M., DíazdeLeón, J.N., Romo-Herrera, J.M., Calva-Yáñez, J.C., Hernández-Lizalde, J.M., Reynoso-Soto, E.A.: Effect of TiO_2 particle and pore size on DSSC efficiency. Mater. Renew. Sustain. Energy (2020). https://doi.org/10.1007/s40243-020-00173-7
25. Zhang, J., Zhou, P., Liu, J., Yu, J.: New understanding of the difference of photocatalytic activity among anatase, rutile and brookite TiO_2. Phys. Chem. Chem. Phys. (2014). https://doi.org/10.1039/c4cp02201g
26. Ghobadi, N.: Band gap determination using absorption spectrum fitting procedure. Int. Nano. Lett. (2013). https://doi.org/10.1186/2228-5326-3-2
27. Boschloo, G., Hagfeldt, A.: Characteristics of the iodide/triiodide redox mediator in dye-sensitized solar cells. Acc. Chem. Res. (2009). https://doi.org/10.1021/ar900138m
28. Molinari, A., Maldotti, A., Amadelli, R.A.: Effect of the electrolyte cations on photoinduced charge transfer at TiO_2. Catal. Today (2017). https://doi.org/10.1016/j.cattod.2016.09.008
29. Lee, C.R., Kim, H.S., Jang, I.H., Im, J.H., Park, N.G.: Pseudo first-order adsorption kinetics of N719 dye on TiO_2 surface. Appl. Mater. Interfaces (2011). https://doi.org/10.1021/am2001696
30. Tsai, J.K., Hsu, T.C., Wu, W.D., Zhou, J.S., Li, J.L., Liao, J.H., Meen, T.H.: Dye-sensitized solar cells with optimal gel electrolyte using the taguchi design method. Int. J. Photoenergy (2013). https://doi.org/10.1155/2013/617126
31. Iwata, S., Shibakawa, S., Imawaka, N., Yoshino, K.: Stability of the current characteristics of dye-sensitized solar cells in the second quadrant of the current-voltage characteristics. Energy Rep. (2018). https://doi.org/10.1016/j.egyr.2017.10.004
32. Cogger, N.D., Evans, N.J.: An introduction to electrochemical impedance measurement. Solartron Analytical Technical Report 6 (2009)
33. Sarker, S., Ahammad, A.J.S., Seo, H.W., Kim, D.M.: Electrochemical impedance spectra of dye-sensitized solar cells: fundamentals and spreadsheet calculation. Int. J. Photoenergy (2014). https://doi.org/10.1155/2014/851705
34. Bisquert, J., Mora-Sero, I., Fabregat-Santiago, F.: Diffusion-recombination impedance model for solar cells with disorder and nonlinear recombination. Chem. Electro. Chem (2013). https://doi.org/10.1002/celc.201300091